



## The Value of Step-by-Step Risk Assessment for Unmanned Aircraft

La Cour-Harbo, Anders

*Published in:*

2018 International Conference on Unmanned Aircraft Systems, ICUAS 2018

*DOI (link to publication from Publisher):*

[10.1109/ICUAS.2018.8453411](https://doi.org/10.1109/ICUAS.2018.8453411)

*Publication date:*

2018

*Document Version*

Early version, also known as pre-print

[Link to publication from Aalborg University](#)

*Citation for published version (APA):*

La Cour-Harbo, A. (2018). The Value of Step-by-Step Risk Assessment for Unmanned Aircraft. In *2018 International Conference on Unmanned Aircraft Systems, ICUAS 2018* (pp. 149-157). [8453411] IEEE. International Conference on Unmanned Aircraft Systems (ICUAS) <https://doi.org/10.1109/ICUAS.2018.8453411>

### General rights

Copyright and moral rights for the publications made accessible in the public portal are retained by the authors and/or other copyright owners and it is a condition of accessing publications that users recognise and abide by the legal requirements associated with these rights.

- Users may download and print one copy of any publication from the public portal for the purpose of private study or research.
- You may not further distribute the material or use it for any profit-making activity or commercial gain
- You may freely distribute the URL identifying the publication in the public portal -

### Take down policy

If you believe that this document breaches copyright please contact us at [vbn@aub.aau.dk](mailto:vbn@aub.aau.dk) providing details, and we will remove access to the work immediately and investigate your claim.

# The Value of Step-by-Step Risk Assessment for Unmanned Aircraft

Anders la Cour-Harbo<sup>1</sup>

**Abstract**—The new European legislation expected in 2018 or 2019 will introduce a step-by-step process for conducting risk assessments for unmanned aircraft flight operations. This is a relatively simple approach to a very complex challenge. This work compares this step-by-step process to high fidelity risk modeling, and shows that at least for a series of example flight missions there is reasonable agreement between the two very different methods.

## I. INTRODUCTION

### A. Background

In 2016 and 2017 EASA (European Aviation Safety Agency) published proposals for legislation [1], [2], [3] on unmanned aircraft in European airspace. This can reasonably be expected to be a reliable precursor for a European legislation in late 2018 or in 2019. This (coming) legislation has adopted the JARUS (Joint Authorities for Rulemaking on Unmanned Systems) proposal for three categories of unmanned aircraft; Open, Specific, and Certified. This categorization is largely risk-based, and while the Open category relies on limitations and operational rules, the Specific and Certified categories rely on risk assessments to be made. These assessments must address both air risk (collision with a manned aircraft or another UA) and ground risk (collision with persons or critical infrastructure). According to EASA [1, p. 5] this risk assessment ‘will incorporate [...] the specific operations risk assessment (SORA), a methodology developed by JARUS for the risk assessment required for UAS operations in the Specific category.’

The SORA was published in a first version by JARUS on April 1, 2018 [4] [TO REVIEWERS: This reference [4] is to the draft version; I will refer to the final version in the camera-ready submission of the paper]. The basic concept of the SORA is a step-by-step process for breaking down the complicated task of conducting a risk assessment for a given flight operation, ending in a ‘Specific Assurance and Integrity Level’ that determines the necessary preparations, documentations, and mitigations necessary for the flight operation to achieve an acceptable level of risk.

This work focuses on how accurate such a discretization of the risk assessment really is, and if the step-by-step approach reasonably can be expected to provide a reliable risk assessment.

### B. Previous work

There are numerous works on how to conceptually approach the challenge of determining the risk of an unmanned aircraft flight. Such works typically borrow from the world of

manned aviation where risk management has been practiced for decades. A number of examples of risk assessments and quantifications for unmanned aircraft include the following. A probabilistic approach to midair collisions is found in [5], where separation of aircraft over the North Atlantic is discussed, and in [6], where a Monte Carlo simulation model is used. [7] takes a combined first principle and stochastic approach to midair collision modeling. A model for vertical separation of manned aircraft is presented in [8]. In [9] a method for determining a no-thrust flight trajectory to reach a particular landing spot is presented. The uncontrolled descent of unmanned aircraft into populated areas have been the subject in a number of publications. This includes [10] that investigate larger aircraft through an equivalent level of safety analysis. [11] specifically looks at distribution of possible impact positions based on simulation, and [12] uses a standard statistical setup and applies a normal distribution approach using aircraft glide parameters to model the impact position. In [13] a comprehensive description of how to manage the risk of unmanned aircraft operations, including ‘the systematic application of management policies, procedures and practices to the activities of communicating, consulting, establishing the context, and assessing, evaluating, treating, monitoring and reviewing risk.’ The barrier bow tie model also used in manned aviation risk assessment is presented in [14]. [15] addresses the lack of an accepted framework and provides some guidelines for how to apply existing models to manage the risk. An study on the impact area for a general uncontrolled descent, including a buffer zone, is presented in [16]. Metrics for safety, including hazard metrics and risks metrics are presented in [17], in [18] a software safety case is developed, and in [19] a generic safety case is presented based on experience with NASA unmanned aircraft missions. A method for automatically finding a proper landing area for an aircraft in emergency descent is shown in [20], [21], and the ability of a fixed wing aircraft to glide to a designated emergency landing area is presented in [22]. In [23] a study for ground impact fatalities resulting from power failure and subsequent uncontrolled glide is presented. An overview in [24] gives a thorough analysis of a variety of ground impact models.

### C. Current work

The purpose of this work is to evaluate the use of the SORA step-by-step procedure for assessing the risk, against the concept of modeling the risk using a high fidelity risk model (HFRM). No new approach and no new model will be presented in this work. The basic assumption is that a model with adequate resolution and details will be able to reliably

<sup>1</sup> Aalborg University, Dept. of Electronic Systems, Fredrik Bajers Vej 7C, 9220 Aalborg East, Denmark.

TABLE I  
PARAMETER VARIATIONS FOR COMPARATIVE STUDY

Parameter	Value 1	Value 2
Type of aircraft	HEF32 20 kg rotorcraft	Cumulus One 2 kg fixed wing
Overflowed area	Partly urban	Rural
Parachute	Yes	No

predict the risk for a given flight scenario. The question to be answered is if the comparatively crude approach of the SORA has sufficient value to reproduce the modeled-based assessment.

Since a full comparison between the SORA and model approaches would be quite extensive and well outside the scope of a single paper, we will focus on a set of particular flight scenarios in the Specific category. This will obviously not fully satisfy the claim that a step-by-step process and a model based approach are equally valid, but it would serve to demonstrate the potential of simplifying a high-fidelity model into an easier to grasp approach.

## II. METHODS

This work is divided into three main sections, starting with this section on the SORA and HFRM methods. Then in Section III the SORA and HFRM are applied to a series of flight scenarios to establish a means for comparison, and the actual comparison is done in Section IV.

This section starts in Subsection II-A with discussing the flight scenarios forming the basis of the comparison, followed by Subsections II-B and II-C with details on the SORA and HFRM methods. Finally, in Subsection II-D fatality rate is introduced as the comparison metric.

### A. Flight scenarios

To have a meaningful result we have chosen to compare the SORA and HFRM using 8 different scenarios all based on an 80 km BVLOS flight operation and generated by varying 3 distinct parameters shown in Table I. All 8 variations take different paths in the SORA method, and all 8 can be specifically addressed in the HFRM. Each variation is therefore a scenario where SORA and HFRM can be independently compared.

1) *Type of aircraft*: Two somewhat different types of aircraft are considered; the HEF32 from Higheye and the Cumulus One from Sky-Watch. Both have sufficient endurance and flight capabilities to conduct the flight, but are otherwise quite different. The Cumulus One in general is an aircraft with an assurance and integrity level equivalent of SAIL II in the SORA, while the HEF32 is at SAIL II to IV, varying over Human Error, Technical Issues, and Adverse Operating Conditions. As the manufacturer (Higheye) as well as the research group behind this paper is working towards SAIL IV overall we will assume this to be the case for this work.

2) *Overflowed area*: A flight path covering about 20% urban area has been chosen as flight path 1. This path has then been altered to avoid any urban areas, resulting in flight path 2. Both flight paths and the population density is shown

TABLE II  
STEPS OF THE SORA PROCESS (FROM [4]).

Purpose	Steps	Outcome
ConOps	0-1	Foundation for assessment
Ground risk	2-5	SAIL value
Air risk	6-9	SAIL value
Threat barriers	10	Measures to take
Check and verification	11-12	Ensuring proper assessment

in Figure 1. Flight path 1 is about 83 km, while path 2 is about 85 km. Care has been taken to change as little as possible, such that the two flight paths are comparable despite their differences.

3) *Parachute*: An emergency recovery capability is considered a significant asset for an unmanned aircraft, and both aircraft are fitted with this; the HEF32 carries a parachute on top of the rotor head, while the Cumulus One aircraft is able to enter a stable deep stall equilibrium, and in this configuration the aircraft descends as if attached to a parachute.

### B. Specific Operations Risk Assessment (SORA)

The SORA is conducted through a total of 13 steps that are detailed in the SORA document from JARUS [4]. An overview of the steps are seen in Table II, and this work will focus on the steps for air and ground risk. Based on the ConOps (Concept of Operations) for the aircraft and its intended mission, two parallel assessments are made for ground and air risk, respectively. The ground risk depends on the type of ground overflowed and the size of the aircraft, while the air risk depends on the type of airspace and the tactical mitigations available. Each assessment ends with a Specific Assurance and Integrity Level (SAIL) ranging from 0 to 6, and the highest one is used in the threat barriers step, where this SAIL is used to determine the type and level of threat barriers necessary to allow flight operations. The SORA steps are relatively clear and unequivocal, with only minor room for interpretations, and as such provide a risk assessment that does not require substantial knowledge of how to determine risks and necessary measures to mitigate them.

### C. High-fidelity modeling of risks

An alternative to the step-by-step process is a detailed modeling of the flight mission based on the ConOps and the parameters for the aircraft. This approach is a likelihood estimation of chain of events that lead to a fatality, and a number of models exist for both ground and air risk estimations (see Section I-B). In this work we will use previous works by the author developed specifically to conduct a quantitative risk assessment that is comparable to the SORA process. For the ground risk the model from [25] will be used, and for the air risk the model from [26] will be used.

We will follow the methods as laid out in the referenced works, and both contain detailed examples to explain how the methods work, also in the setup used in this work. As such, there will be no detailed explanation of these methods here.

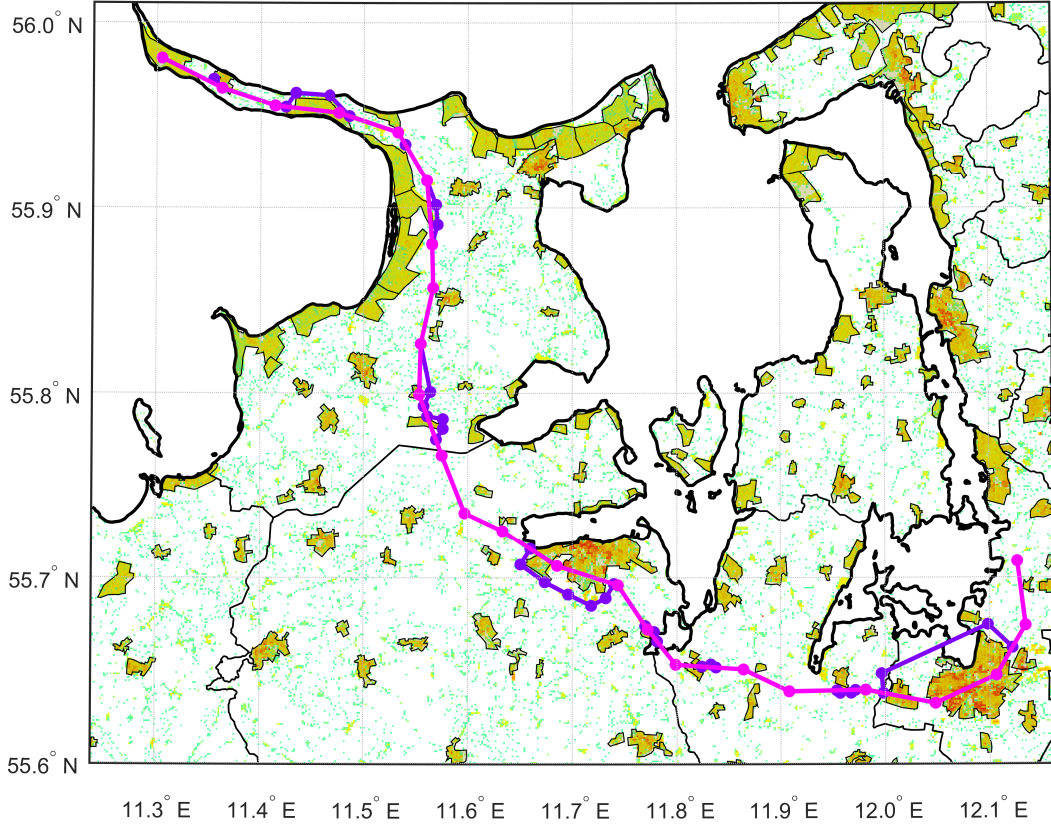


Fig. 1. The flight path 1 (light purple) follows an imaginary pipeline in need of inspection. It passes through both rural and urban areas. It starts at the lower right close to Roskilde, and goes over Holbæk halfway, and ends at Sjællands Odde. Flight path 2 (dark purple) is the original flight path altered to avoid urban areas, but still follow the pipeline (as much as possible). Path 1 and 2 are about 80% identical, differing only where there is urban areas overflow. Path 2 simply circumvents any urban area overflow with path 1. The population density is shown as white (density 0) over light green, green, orange to red for increasing density, with a resolution of  $100 \text{ m} \times 100 \text{ m}$ . The green patches are topographical indications of officially recognized urban areas.

#### D. Comparison using fatality rate

The comparison metric between SORA and HFRM is done via the fatality rate, which in some sense is the ultimate goal of any risk assessment. That is, if the assessment concludes that the fatality rate is sufficiently low, the mission can be conducted. The question to be addressed in this work essentially is if the fatality rate from the SORA and the modeled approaches line up for the same missions.

In the SORA the starting point is a desired maximum fatality rate, and the entire process is intended to determine the necessary procedures, barriers, and mitigations to achieve this. In the model approach it is the opposite, in the sense that given all parameters for a particular mission, the fatality rate can be determined.

The SORA states that 'The objective for the number of fatal injuries to third parties on the ground (per flight hour) comes from a principle of equivalence with the manned aviation [...] [4, p. 21], but does not specifically provide a quantification of this. It is indicated that a level of  $10^{-6}$  fatalities per flight hour would be acceptable, although this is rather high compare to at least commercial aviation [13]. However, for this work we will stick with this number for

the sake of comparison.

### III. APPLYING METHODS

The SORA and HFRM methods are now applied to the 8 flight scenarios. First, in Subsection III-A the SORA is applied to the ground risk, following by the HFRM applied to the ground risk in Subsection III-B. The probabilities associated with malfunctions of the aircraft are discussed in Subsection III-C, and the HFRM output is then presented in Subsection III-D.

Then the SORA air risk is processed in Subsection III-E followed by a brief review of the resulting threat barriers in Subsection III-F. Then in Subsection III-G the HFRM for air risk is presented.

#### A. Determining the ground risk using SORA

The steps #2 through #5 is for determining the risk associated with ground impacts [4].

*Step #2: Determination of the intrinsic Ground Risk Class*  
The first parameter for determining the Ground Risk Class (GRC) is the 'UAS lethal area' and the intended type of operation. The former is quantified through the 'max UAS characteristic dimension' which for the Cumulus aircraft is

TABLE III  
GROUND RISK CLASSES FOR SORA

Intrinsic UAS Ground Risk Class		
Max UAS dimension	1 m < 700 J	3 m < 34 kJ
Operational scenario for aircraft	Cumulus	HEF
BVLOS over populated environment Flight path 1	6	7
BVLOS over sparsely populated area Flight path 2	2	3
Final UAS Ground Risk Class		
Flight path 1 After applying harm barriers	4	6
Flight path 2 After applying harm barriers	0	2

1.65 meter, putting the aircraft in the '3 m' category (Figure 8 in the SORA) with an expected kinetic energy of < 34 kJ. However, the actual kinetic energy of the aircraft, at mass 2 kg and cruise speed 16 m/s, is around 250 J, well below the expected max value of 700 J for the smaller < 1 m category. Therefore, the 1 m category is appropriate. The HEF32 has rotor diameter of 1.82 m, and kinetic energy at cruise speed of approximately 10 kJ. This puts it in the '3 m' category.

The second parameter for determining GRC is 'Operational scenario'. For the partially urban scenario this will be category 'BVLOS over populated environment', while the purely rural scenario is category 'BVLOS over sparsely populated environment'. This results in the GRC values listed in Table III.

#### Step #3: Identification of harm barriers

Three harm barriers are listed in Table 2 of the SORA. For the first barrier we will assume the existence of a Medium integrity Emergency Response Plan (ERP). For the second barrier both aircraft are equipped with means of reducing the ground impact effects. Since the HEF is still capable of causing a fatality in a parachuted descent, the robustness will be set to Medium, while for the Cumulus the deep stall descent has been proven non-lethal, and thus qualifies as robustness High. For the third barrier there is no effect in the presented scenarios. Following Table 2 in SORA this gives a reduction of the GRC by 1 for the HEF32 and by 2 for the Cumulus.

#### Step #4: Lethality determination

The SORA does not provide much detail on lethality determination. In fact, the lethality is simple quantified as 'average' if there is neither extenuating nor aggravating circumstances for the aircraft.

#### Step #5: SAIL determination

Determining the Specific Assurance and Integrity Level (SAIL) is the last step in the ground impact assessment. This is done using Table 4 in SORA, and the result is shown in Table IV.

#### B. Determining the ground risk using HFRM

The model for ground fatalities is a stochastic model that joins probabilities in the causal chain from drone malfunction

TABLE IV  
GROUND IMPACT SPECIFIC ASSURANCE AND INTEGRITY LEVEL BASED ON TABLE 4 IN SORA.

Operational scenario for aircraft	SAIL	
	Cumulus	HEF
Flight path 1 Without parachute/deep stall	V	VI
Flight path 2 Without parachute/deep stall	I	II
Flight path 1 With parachute/deep stall	III	V
Flight path 2 With parachute/deep stall	0	I

to a potential fatality, and is based on the model in [25]. It takes the form

$$P_{\text{fatality}} = p_{\text{event}} \cdot p_{\text{impact person}} \cdot p_{\text{fatal impact}}, \quad (1)$$

where  $p_{\text{event}}$  is the probability per time of a given event (of which we will use four),  $p_{\text{impact person}}$  is the conditional probability that given an occurrence of one of the events that a person will be impacted as a result, and  $p_{\text{fatal impact}}$  is the conditional probability that this person suffers a fatal injury.

The four events are ballistic descent, uncontrolled glide, parachute-like descent, and flyaway. These event types, including how they are modeled, are described in more detail in [25], [27], [28].

This HFRM uses a rather large set of parameters due to the complicated and detailed nature of the descent models. In addition to the few variations listed in Table I, the first principles HFRM parameters used for the modeling are listed in Table V. The computational parameters for discretization and numerical integration are similar to those used in [25] and are not repeated here.

#### C. Event probabilities

The event probabilities  $p_{\text{event}}$  are listed in Table VI. These are crucial parameters in the sense that they relate indirectly to the level of assurance and integrity of the aircraft and their operations as described in the SORA. The numbers listed here are NOT actual numbers for the two aircraft (to the best of the author's knowledge those numbers are not known), but are rather expressions of conservative estimates based on the quality of the aircraft parts (mechanics and electronics), associated pilot training, available procedures for normal, abnormal, and emergency situations, availability of documentation to operators, maintenance procedures, autopilot flight hours, etc. In fact, the event probabilities are directly dependent on the threat barriers listed under Step #10 in the SORA (see Section III-F), and the probabilities listed in Table VI are derived from a Cumulus One at SAIL II and HEF32 at SAIL IV.

Note that for the rotorcraft an uncontrolled glide is considered a descent, where the aircraft has lost some of its lift (for instance due to a malfunctioning actuator) and will descent fairly quickly with rotor still spinning.

TABLE V  
HFRM PARAMETERS (SEE [25] FOR USE)

Parameter	Cumulus	HEF32
Flight time	2.5 h	4.5 h
Mass	2 kg	20 kg
Cruise speed	16 m/s	18 m/s
Glide speed	12 m/s	16 m/s
Glide ratio	$N(10, 2)$	$N(3, 0.5)$
Drag coef for ballistic	$N(0.9, 0.2)$	$N(0.7, 0.2)$
Drag area for ballistic	0.02 m <sup>2</sup>	0.1 m <sup>2</sup>
Person impact area ballistic	25 cm <sup>2</sup>	100 cm <sup>2</sup>
Person IA parachute/deep stall	0.5 m <sup>2</sup>	0.3 m <sup>2</sup>
Person IA glide/fly-away	50 cm <sup>2</sup>	144 cm <sup>2</sup>
Drag coef parachute/deep stall	$N(0.94, 0.1)$	$N(1.13, 0.2)$
Drag area parachute/deep stall	0.5 m <sup>2</sup>	12.57 m <sup>2</sup>
Parameters	Path 1	Path 2
Flight distance	81 km	83 km
Flight altitude	75 m	75 m
Number of WPs	23	53
Wind speed	$N(1, 0.4) / N(5, 2) / N(9, 3.6)$	
Wind direction	$N(0, 0.17)$ [from west]	
Flyaway – long short ratio	0.01	
Flyaway – short distance sigma	4000 m	

TABLE VI  
EVENT PROBABILITIES (EVENTS PER HOUR).

	Ballistic	UG	Parachute	Flyaway
HEF parachute	1/700	1/600	1/150	1/1000
HEF no parachute	1/210	1/200	n/a	1/1000
Cumulus deep stall	1/150	1/120	1/40	1/100
Cumulus no deep stall	1/52	1/48	n/a	1/100

The parachute/deep stall event is meant to ‘capture’ some of the ballistic and uncontrolled glide events, that is, the parachute/deep stall will be initiated in some of the cases where the aircraft would otherwise have descended ballistically or uncontrolled. It follows that when there is no such emergency recovery capability available (the no-parachute option in Table I) the probability has been shifted (equally) to the ballistic and uncontrolled glide events. Consequently, the total probability for ballistic, uncontrolled glide, and parachute is the same with and without parachute/deep stall.

#### D. HFRM model output

The results of using ground impact HFRM on all 8 scenarios is shown in Figure 2. In addition to the scenarios the wind speed is also varied, because it plays a significant role in the descent models. In particular, a parachute/deep stall descent has a much higher impact speed (and thus lethality) if the wind is higher. This feature is not captured in any way in the SORA, but included here to see what impact it has. It is important to note that while HFRM produces seemingly very accurate fatality rates, one should focus only on the order of magnitude of the results, since the numbers will invariably change with adjustments to any of the many parameters, some of which are purely educated guesses (see [25] for discussion of this topic).

#### E. Determining the airspace encounter risk using SORA

The steps #6 through #9 is for determining the risk associated with airspace encounters.

TABLE VII  
AIR RISK VALUES FOR SORA

Scenario	Partly urban	Rural
AEC	9	10
Initial ARC	3	2
Intermediate ARC	3	2
Operational Restrictions	3	2
Final ARC	3	2
Structures and Rules	3	2
SAIL	IV	II
Uncontained ARC	3	3
Recommended max loss of containment rate	10 <sup>-3</sup> per hour	10 <sup>-3</sup> per hour
Tactical Mitigation Performance Requirement	Medium	Low
Detection level for DAA system	90%	50%

*Step #6: Determination of the Airspace Encounter Category*  
There are 12 AECs in the SORA. The only variations in scenarios in this work that affects the AEC is whether the flight is (partly) over urban or rural areas. For urban areas (flight path 1) the AEC is 9, which reads ‘Operations below 500 ft. AGL within Uncontrolled Airspace over urban environment’, and for rural areas (flight path 2) the AEC is 10, which reads ‘Operations in Class G airspace below 500 ft. AGL over Rural environment’.

#### Step #7: Initial Air-Risk Class (ARC) Assignment

The initial ARC follows directly from the AEC using Table 5 in SORA. The result is shown in Table VII.

#### Step #8: Identification of the Strategic Mitigations

There are no strategic mitigations of any kind in any of the listed scenarios. It is possible to use a study of the traffic density in the target airspace, but the SORA provides no guidelines for this. As this is a comparative study with just such a method, it would defy the purpose to use the HFRM to determine traffic density. As such, neither the ‘operational restrictions’ nor ‘structures and rules’ mitigative means will reduce the initial ARC. The resulting SAIL follows from Table 6 in SORA, and the result is listed in Table VII.

The last part of this step is determining the Uncontained ARC, i.e. ARC of areas adjacent to the flight path. Since all flights are close to urban areas the adjacent airspace is regularly through both flight paths AEC 9 with ARC 3. In addition, the flight paths pass just outside the controlled airspace of Roskilde Airport (EKRK). The AEC for this airspace is AEC 8 for which the ARC is also 3. Consequently, SORA recommends means that ensure that breach of containment is less likely than 1 per 1000 flight hours.

#### Step #9: Tactical Mitigation Performance Requirement (TMPR) Assignment

Tactical mitigation allows for short term or on-the-fly mitigation. Following the determination of final ARC the TMPR are assigned as listed in Table VII, and according to Annex C in the SORA, these TMPR levels give raise to a minimum capability of the Detect and Avoid system used.

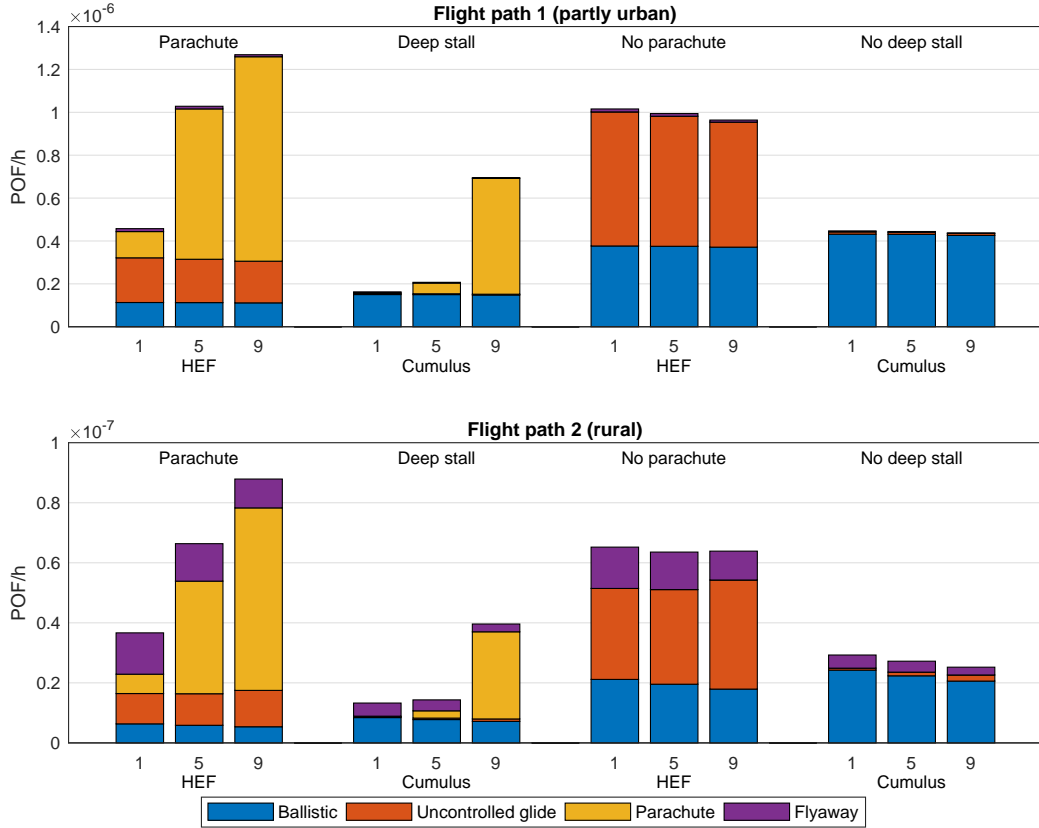


Fig. 2. Result of using HFRM on all 8 flight scenarios. For each scenario 3 different wind speeds were used (1, 5, and 9 m/s, see Table V) since this affects the parachute/deep stall fatality rate somewhat. The height of each bar shows the total rate (probability of fatality per flight hour), and each bar also shows how the rate is composed from the four different modeled descent events. Note that the second axis is an order of magnitude smaller for the rural flight path compared to the urban flight path.

#### F. Identification of recommended threat barriers (Step #10)

The threat barriers needed to allow flight operations to commence can now be determined as step #10 using Table 9 in the SORA. The barriers required for each of the 8 scenarios should, if the SORA and HFRM methods line up, be precisely those that produces the event probabilities listed in Table VI. This will be examined in the Results in Section IV.

Step #11 and Step #12 are revisions of the risk assessment, and will no be addressed in this work.

#### G. Determining the airspace encounter risk using HFRM

The model for airspace encounter risk is based on the model presented in [26]. It models the fatality rate for impacts between a general aviation (GA) aircraft (such as smaller fixed wing, rotorcraft, hang gliders, ultra lights, etc), and an unmanned aircraft (UA). It is composed of three probabilistic parts that are assumed independent, plus two factors to account for mitigations and lethality. The model is

$$r_{\text{fatality}} = p_{\text{hi}} \cdot p_{\text{vi}} \cdot p_{\text{below}} \cdot \lambda_{\text{stm}} \cdot p_{\text{fatality}} \cdot \quad (2)$$

The first term  $p_{\text{hi}}$  is the probability of 'horizontal impact' based on the speeds of the GA and the UA, and is probability per time unit. The second term  $p_{\text{vi}}$  is the probability of

'vertical impact', which is based on probability density functions for the altitude of both aircraft, as well as the height of both aircraft. The third term  $p_{\text{below}}$  is the probability that the GA is below 100 meter, the general maximum flight altitude in Denmark. The fourth term  $\lambda_{\text{stm}}$  is the effect of strategic and tactical mitigations. For an in-depth description of the terms, see [26].

The fifth term  $p_{\text{fatality}}$  is the probability of one fatality as a consequence of impact. This term is not part of the original impact model, but is specifically included here to accommodate the comparison with the SORA (as described in Section II-D).

The majority of the parameters in this model are air traffic densities and first principle parameters for 9 different types of aircraft. For this work, these are chosen identical to the parameters in [26]. In addition, the parameters for the two unmanned aircraft in this work, HEF32 and Cumulus One, are shown in Table VIII.

The parameters for strategic/tactical mitigation and lethality are listed in Table IX. When  $\lambda_{\text{stm}} = 1$  there is no mitigation, which is the case for most GA. However, since the HEF32 is equipped with FAR23 compliant navigation and anti-collision lighting, which makes the aircraft easier to see for GA, also during daytime operations (see CFR



TABLE VIII

PARAMETERS FOR THE AIRCRAFT FOR AIRSPACE ENCOUNTER HFRM.

Parameter	Cumulus	HEF
Altitude distribution	$N(75, 8)$	$N(75, 8)$
Safety radius	1.65 m	1.90 m
Cruise speed	16 m/s	18 m/s
Aircraft height	0.3 m	0.9 m

TABLE IX

STRATEGIC MITIGATION AND LETHALITY PARAMETERS FOR AIRSPACE ENCOUNTER HFRM.

Parameter	Cumulus		HEF	
	S/T mitigation $\lambda_{sm}$	Lethality $p_{fatality}$	S/T mitigation $\lambda_{sm}$	Lethality $p_{fatality}$
Fixed wing	1	1	0.8	1
Rotorcraft	1	1	0.5	1
Glider	1	0.5	1	1
Motor glider	1	0.5	1	1
Ultra light	1	1	1	1
Hang glider	1	1	1	1
Paraglider	1	1	1	1
Parachute	1	1	1	1
Balloon	0.01	0.5	0.01	2

§23.1401 - Anti-collision light system), lower values have been used for fixed-wing and rotorcraft. The assumption is that such lighting will indeed lower the probability of collision with 20% and 50%, respectively, since pilots of such GA aircraft can be presumed to observant for other air traffic, and recognize anti-collision lighting. More so for rotorcraft which typically will be flying relatively slow at very low altitudes. In addition, a strategic mitigation for balloons is set very low, assuming that balloons are operated in known locations, and at known times. The basis for this assumption is detailed in [26].

Lethality is set to 1 for most GA (meaning that on average one fatality will result from a midair collision). However, given the small mass of the Cumulus One aircraft and the relatively low speed of gliders on approach (which is most likely the case below 100 meter) the lethality for gliders is set to 0.5. Also, assuming that the Cumulus will most likely not damage a balloon to the point where it will descent rapidly, the balloon lethality is also at 0.5. On the other hand, the HEF32 will very likely significantly crippled a balloon, and assuming more than one person in the balloon basket, the lethality is set to 2.

The result of applying all of the above parameters to the HFRM for airspace encounters is shown in Figure 3. The model does not directly support distinctions between rural and urban airspace, and as such the results as shown apply equally to both types of airspace.

#### IV. RESULTS

The previous section contains a series of outputs from the SORA and the HFRM, and the aim in this section is to compare these outputs to evaluate the step-by-step SORA process.

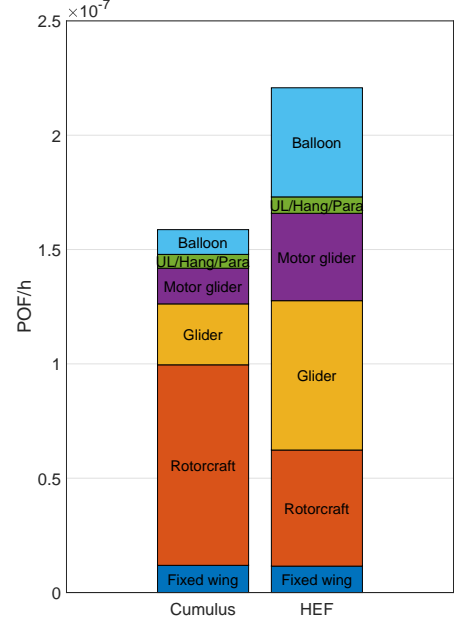


Fig. 3. The probability of fatality from a midair collision based on the HFRM in (2). Results are shown for both unmanned aircraft. The total probabilities are  $1.6 \cdot 10^{-7}$  fatalities per flight hour for the Cumulus and  $2.2 \cdot 10^{-7}$  fatalities per flight hour for the HEF. The probabilities related to the 9 types of GA are also shown.

TABLE X  
FINAL SAIL.

Operational scenario for aircraft	SAIL	
	Cumulus	HEF
Flight path 1 (urban) Without parachute/deep stall	V	VI
Flight path 2 (rural) Without parachute/deep stall	II	II
Flight path 1 (urban) With parachute/deep stall	IV	V
Flight path 2 (rural) With parachute/deep stall	II	II

The final SAIL for the SORA is obtained by combining the SAIL in Tables IV and VII. The result is shown in Table X, where the lower value of II is originating in the midair collision risk, and the upper values of IV to VI originate in the ground impact risk.

At the same time it was shown using high-fidelity modeling that the ground fatality rate as well as the midair collision fatality rate in all 8 scenarios were around or below  $10^{-6}$  fatalities per flight hours, as seen in Figures 2 and 3. It is important to note that the values depicted in Figure 2 are averages over the entire flight. Since the flight paths are 80% the same, the one magnitude of overall different between urban and rural are in fact caused by 'only' the 20% difference in flight path. This is because the POF for the urban parts of the flights often raises to  $10^{-5}$  and occasionally even higher.

The first concluding observation is that both the Cumulus SAIL II aircraft and the HEF SAIL IV aircraft achieve (in



SORA terms) very acceptable POF per flight hour in the rural flight scenarios. However, for the urban scenarios the POF is only just acceptable for the HEF, though slightly better for the Cumulus, and only because the majority of the flight is over rural areas that contribute significantly to reduce the average POF. For a purely urban flight both aircraft would exceed the  $10^{-6}$  POF, the HEF with roughly on order of magnitude, and the Cumulus with a factor of 2 or 3 (this is not visible from any presented figure, but it is clear from the detailed modeling output).

The second concluding observation is that the final SAIL values partly corroborates the first concluding observation: From Table X we see that the required SAIL for all rural flights is II, thus according to the SORA both Cumulus and HEF are acceptable for the rural flights. It also follows from the table that none of the urban flights can be conducted with the present aircraft. Even though the SAIL IV HEF32 may seem close to the SAIL V requirement for urban flight (with parachute), the actual step from SAIL IV to SAIL V is quite large, and not realistically achievable with the current HEF32 aircraft.

Additionally, it is noticeable that while the SORA considers a parachute a significant reduction in risk (by allowing for one full GRC point to be subtracted) this effect is not nearly as significant for the HFRM approach. This is because the kinetic energy on impact is still quite large, especially if the aircraft in addition to the vertical descent is moving horizontally with a significant speed due to wind. In the modeled scenario the shelter factor for the parachuted descent is double that of the shelter factor for other descents, based on the assumption that there is a 50% chance of spotting the descending aircraft when it is hanging from a parachute. This may be set somewhat too low, though.

## V. CONCLUSIONS

Overall, the step-by-step process of the SORA approach and the detailed modeling of HFRM approach seems to be largely in agreement. The methods are hugely different and any metric for comparison is bound to be less than perfect, and the uncertainty associated with these risk assessments due to lack of exact knowledge and historical flight data to backup assumptions only adds to the overall impression that the two methods generally align fairly well despite the obvious points of misalignment.

The hope that the much simpler SORA approach can generally capture sufficient details to provide reliable and trustworthy risk assessment seems justified, at least to the extend covered by the flight scenarios presented in this work.

## REFERENCES

- [1] European Aviation Safety Agency, "Notice of Proposed Amendment 2017-05 (A) - Introduction of a regulatory framework for the operation of drones," Tech. Rep., 2017.
- [2] —, "Notice of Proposed Amendment 2017-05 (B) - Introduction of a regulatory framework for the operation of drones," Tech. Rep., 2017. [Online]. Available: [https://www.easa.europa.eu/sites/default/files/dfu/NPA\\_2017-05\(B\).pdf](https://www.easa.europa.eu/sites/default/files/dfu/NPA_2017-05(B).pdf)
- [3] —, "“Drone Collision” Task Force. Final Report," European Aviation Safety Agency, Tech. Rep., oct 2016.
- [4] JARUS, "JARUS guidelines on Specific Operations Risk Assessment (SORA)," Joint Authorities for Rulemaking of Unmanned Systems JARUS, Tech. Rep., 2017. [Online]. Available: [http://jarus-rpas.org/sites/jarus-rpas.org/files/jar\\_doc\\_06\\_jarus\\_sora\\_v1.0.pdf](http://jarus-rpas.org/sites/jarus-rpas.org/files/jar_doc_06_jarus_sora_v1.0.pdf)
- [5] R. E. Machol, "An Aircraft Collision Model," *Management Science*, vol. 21, no. 10, pp. 1089–1101, jun 1975.
- [6] R. W. Patlovany, "U.S. aviation regulations increase probability of midair collisions," *Risk Analysis*, vol. 17, no. 2, pp. 237–248, 1997.
- [7] S. Endoh, "Aircraft Collision Models," MIT Flight Transportation Laboratory, Tech. Rep., may 1982.
- [8] J. M. Richie, "Description of the Derivation of the Collision Risk Model Used in the vertical separation Simulation Risk Model (DOT/FAA/CT-TN88/38)," Federal Aviation Administration, Tech. Rep., feb 1989.
- [9] E. M. Atkins, I. A. Portillo, and M. J. Strube, "Emergency Flight Planning Applied to Total Loss of Thrust," *Journal of Aircraft*, vol. 43, no. 4, pp. 1205–1216, jul 2006.
- [10] D. W. King, A. Bertapelle, and C. Moses, "UAV Failure Rate Criteria for Equivalent Level of Safety," in *International Helicopter Safety Symposium*, Montreal, 2005, p. 9.
- [11] P. Wu and R. Clothier, "The Development of Ground Impact Models for the Analysis of the Risks Associated with Unmanned Aircraft Operations Over Inhabited Areas," in *Proceedings of the 11th Probabilistic Safety Assessment and Management Conference (PSAM11) and the Annual European Safety and Reliability Conference (ESREL 2012)*, 2012, p. 14.
- [12] R. Clothier, R. Walker, N. Fulton, and D. Campbell, "A casualty risk analysis for unmanned aerial system (UAS) operations over inhabited areas," in *Second Australasian Unmanned Air Vehicle Conference*, 2007, pp. 1–15.
- [13] R. A. Clothier and R. A. Walker, "The Safety Risk Management of Unmanned Aircraft Systems," in *Handbook of Unmanned Aerial Vehicles*, K. P. Valavanis and G. J. Vachtsevanos, Eds. Springer Science + Business Media B.V., Dordrecht, Netherlands, 2013, p. 37.
- [14] R. Clothier, B. Williams, and A. Washington, "Development of a Template Safety Case for Unmanned Aircraft Operations Over Populous Areas," in *SAE 2015 AeroTech Congress & Exhibition*, sep 2015, p. 10.
- [15] R. A. Clothier, B. P. Williams, and N. L. Fulton, "Structuring the safety case for unmanned aircraft system operations in non-segregated airspace," *Safety Science*, vol. 79, pp. 213–228, 2015.
- [16] G. Guglieri and G. Ristorto, "Safety Assessment for Light Remotely Piloted Aircraft Systems," in *2016 INAIR - International Conference on Air Transport*, 2016, pp. 1–7.
- [17] X. Lin, N. L. Fulton, and M. E. T. Horn, "Quantification of high level safety criteria for civil unmanned aircraft systems," in *IEEE Aerospace Conference Proceedings*, 2014, p. 13.
- [18] E. Denney, G. Pai, and I. Habli, "Perspectives on software safety case development for unmanned aircraft," *Proceedings of the International Conference on Dependable Systems and Networks*, 2012.
- [19] E. Denney and G. Pai, "Architecting a Safety Case for UAS Flight Operations," in *34th International System Safety Conference*, 2016, p. 12.
- [20] M. Warren, L. Mejias, X. Yang, B. Arain, F. Gonzalez, and B. Upcroft, "Enabling Aircraft Emergency Landings Using Active Visual Site Detection," in *Field and Service Robotics*. Springer Tracts in Advanced Robotics 105, 2015, pp. 167–181.
- [21] M. Warren, L. Mejias, J. Kok, X. Yang, F. Gonzalez, and B. Upcroft, "An Automated Emergency Landing System for Fixed-Wing Aircraft: Planning and Control," *Journal of Field Robotics*, vol. 32, no. 8, pp. 1114–1140, dec 2015.
- [22] M. Coombes, W.-H. Chen, and P. Render, "Landing Site Reachability in a Forced Landing of Unmanned Aircraft in Wind," *Journal of Aircraft*, pp. 1–13, feb 2017.
- [23] S. Bertrand, N. Raballand, F. Viguier, and F. Muller, "Ground Risk Assessment for Long-Range Inspection Missions of Railways by UAVs," in *Proceedings of ICUAS 2017*, 2017, pp. 1343–1351.
- [24] A. Washington, R. A. Clothier, and J. Silva, "A review of unmanned aircraft system ground risk models," *Progress in Aerospace Sciences*, vol. 95, no. November, pp. 24–44, 2017.
- [25] A. la Cour-Harbo, "Quantifying ground impact fatality rate for small unmanned aircraft," 2018, preprint.
- [26] A. la Cour-Harbo and H. Schioler, "Modeling probability of midair

collision between general aviation and small unmanned aircraft,” 2018, preprint.

- [27] A. la Cour-Harbo, “Ground impact probability distribution for small unmanned aircraft in ballistic descent,” 2018, preprint.
- [28] —, “Quantifying risk of ground impact fatalities of power line inspection BVLOS flight with small unmanned aircraft,” in *2017 International Conference on Unmanned Aircraft Systems (ICUAS)*, 2017, pp. 1352–1360.